

Mechanical reliability of ceramic windows in high frequency microwave heating devices

Part 1 *An analysis of temperature and stress distributions*

M. K. FERBER, H. D. KIMREY*, P. F. BECHER

*Metals and Ceramics Division, and *Fusion Energy Division, Oak Ridge National Laboratory, Oak Ridge, Tennessee 37830, USA*

The temperature and stress distributions generated in ceramic window materials currently employed in microwave gyrotron tubes were determined for a variety of operating conditions. Face-cooled windows of both polycrystalline BeO and polycrystalline Al₂O₃ were considered. The actual analysis involved three steps. First, a computer program was used to determine the electric field distribution within the window at a given power level and frequency. This program was capable of describing both the radial and axial dependence of the electric field. Second, the field distribution was used to derive an expression for the heat generated per unit volume per unit time within the window due to dielectric losses. A generalized heat conduction computer code was then used to compute the temperature distribution based on the heat generation function. Finally, the stresses were determined from the temperature profiles using a finite-element computer program. Primary emphasis was given to determining the effect of frequency upon the resulting thermal stress distribution. In addition, the effects of increasing window diameter and enhancing heat removal from the windows were considered.

1. Introduction

In recent years, a considerable effort has been directed toward developing microwave tubes capable of producing 200 to 5000 kW of continuous (cw) power at frequencies between 28 and 150 GHz. One particular microwave device, called a gyrotron, has application for electron cyclotron resonance heating (ECRH) in fusion energy systems [1, 2]. As shown in Fig. 1, the output section of the gyrotron contains a ceramic window in the form of a circular plate which is attached to the tube via a metallizing and brazing process. The window, which is used to maintain the internal vacuum of the gyrotron, must be capable of transmitting the microwave energy without significant energy absorption. Commercially available polycrystalline ceramics such as BeO and Al₂O₃ have been successfully used for 28 GHz operation at power levels up to 342 kW into a matched test load. However, in recent 60 GHz experiments, these same materials have experi-

enced a high incidence of fracture. There is evidence that the failures resulted from increases in the temperature gradients and thus the thermal tensile stresses generated during 60 GHz (≥ 100 kW cw) operation.

These observations emphasize the need for reliable estimates of the in-service stresses arising from microwave heating, particularly if a design philosophy is to be established for the window materials. Unfortunately, previous treatments have been based on one-dimensional (1-D) (through-the-thickness) analyses, which neglect the two- and three-dimensional (2- and 3-D) nature of the temperature gradients. As will be shown, this 1-D approach can significantly underestimate the maximum tensile stress. In Part 1 of this paper, the temperature and thermal stress distributions are predicted for various gyrotron operating conditions using more realistic 2- and 3-D treatments. Calculations are presented for both BeO and Al₂O₃ materials. Verification of

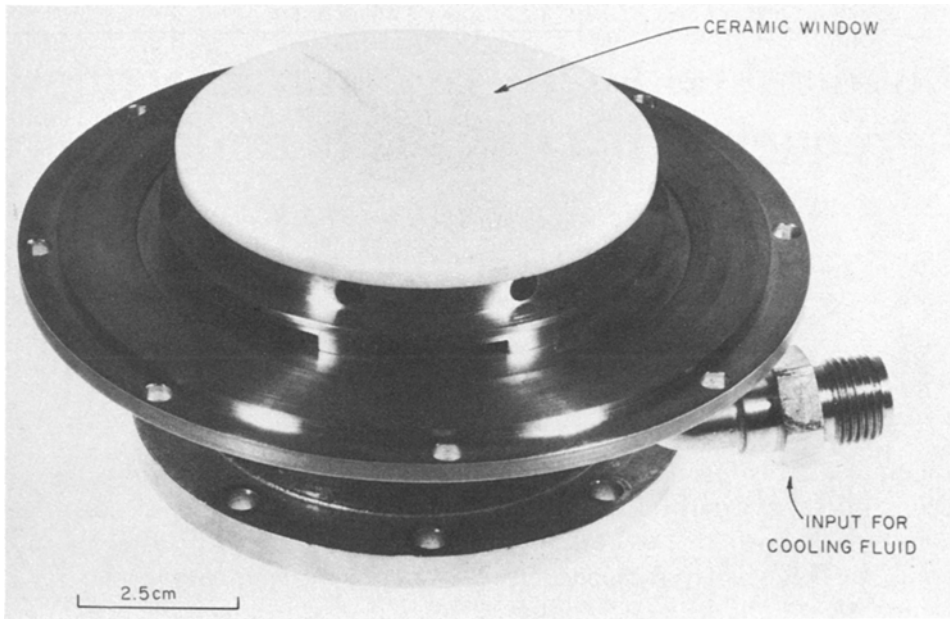


Figure 1 Output section of gyrotron tube illustrating use of ceramic window.

the analysis is given by comparing the locations of potential fracture sites predicted from the calculated stress distributions with experimentally observed failure origins in actual window materials.

In Part 2, results of recent fracture mechanics measurements [3] involving both BeO and Al₂O₃ are presented. These data are used in conjunction with the estimates of maximum tensile stresses to evaluate long-term mechanical reliability of

both BeO and Al₂O₃. Particular attention is given to the possible catastrophic failure of the window resulting from a time-dependent weakening process that is due to growth of pre-existing flaws [4–6].

2. Background

2.1. Window configuration and materials

Fig. 2 illustrates the dual window configuration typically used to provide a continuous output

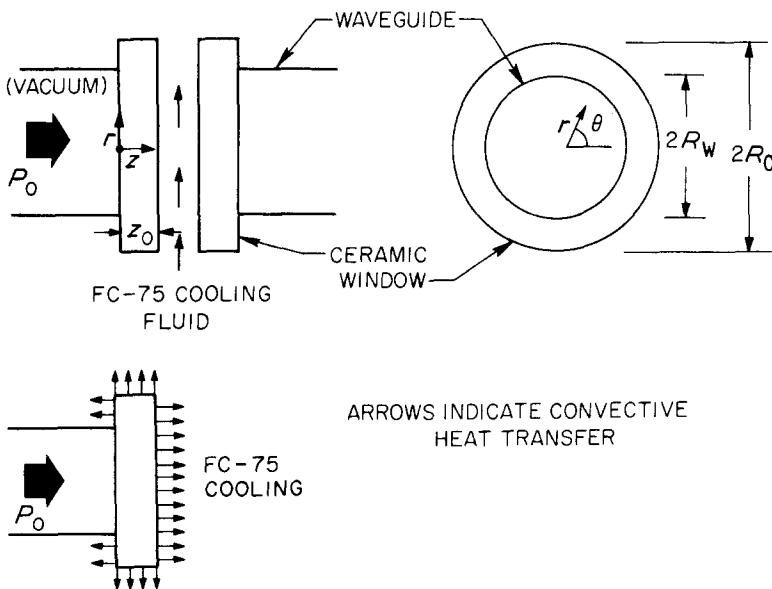


Figure 2 Dual window configuration typically used to provide continuous power output. Details of window geometry are shown in (a) while (b) illustrates assumed cooling conditions resulting from FC-75.

TABLE I Suppliers and physical properties of Al₂O₃ and BeO window materials

Characteristic*	Al ₂ O ₃	BeO
Vendor	Wesgo, Bellevue, California	Brush-Wellman Corporation, Santa Ana, California
Designation	AL995 Al ₂ O ₃	Thermalox 995 standard BeO
Density (g cm ⁻³)†	3.84 (96.4%)	2.904 (96.5%)
Average grain size (μm)	30	35
Thermal conductivity (W cm ⁻¹ °C ⁻¹)		
25° C	0.334	2.52
125° C	0.245	1.82
225° C	0.187	1.35
325° C	0.146	1.03
425° C	0.117	0.81
Specific heat (J g ⁻¹ °C ⁻¹), 25° C	0.775	1.046
Young's modulus (GPa)	385	360
Poisson's ratio	0.25	0.25
Thermal expansion coefficient (°C ⁻¹), 25–500° C	7.5 × 10 ⁻⁶	6.8 × 10 ⁻⁶
Inert fracture strength‡ (MPa)	276 ± 19.3	186.1 ± 16.6
(10 ³ psi)	40.12 ± 2.80	26.99 ± 2.41

*Various physical properties are taken from both vendors' information and data obtained from recent measurements.

†Numbers in parentheses represent percent of theoretical density.

‡Strength values obtained from four-point bend tests conducted in liquid nitrogen. Additional details are given in ref. 3. The numbers following the ± signs are standard deviations.

of microwave energy. During operation of the gyrotron, high electric fields are established within the windows. Because current materials exhibit finite dielectric losses, energy is absorbed and significant quantities of heat can be generated within the window. Face cooling is required so that resulting temperatures and temperature gradients are not excessive. The cooling medium is typically a commercial fluorocarbon liquid (FC-75)*, which is chosen because of its low viscosity and low energy absorption in the microwave frequency range. In this configuration, the heat flow is mainly through the window face exposed to the cooling fluid (Fig. 2b).

As previously stated, the two window materials commonly used in the gyrotron tube are commercially available polycrystalline forms of Al₂O₃ and BeO. Table I lists several important physical properties for each material. It should be emphasized that the fracture strengths reported in Table I should be used only to make relative comparisons. This limitation is necessary since the fracture strength of ceramics can be significantly influenced by several factors including test geometry, stressing rate, environment, specimen size,

surface finish, and microstructural characteristics.† Even if all of these factors are fixed, the strength will generally exhibit considerable variation (note the standard deviations in Table I). Additional details concerning the microstructures of both materials are provided in Part 2.

2.2. Temperature and stress analyses

In general, the steady-state temperature distribution established within a flat, cylindrical window subject to internal heat generation will be a function of the spatial coordinates (r, θ, z). The exact form of the distribution can be determined by solving the general heat conduction equation [7],

$$\frac{\partial^2 T}{\partial r^2} + \frac{1}{r} \frac{\partial T}{\partial r} + \frac{1}{r^2} \frac{\partial^2 T}{\partial \theta^2} + \frac{\partial^2 T}{\partial z^2} + \frac{q'''}{k_t} = 0, \quad (1)$$

where T is the temperature, k_t is the thermal conductivity, and q''' is the heat generation rate per unit volume. For microwave applications, q''' represents the heat generation from dielectric losses and thus can be written as [8]

$$q''' = (\pi f)(\epsilon_r \epsilon_0 \tan \delta) |E_p|^2, \quad (2)$$

*Product of 3M Company, St. Paul, Minn.

†The strength data in Table I minimize effects of stressing rate and environment since tests were conducted in liquid nitrogen (see [3]).

where f is the frequency, ϵ_r is the relative dielectric constant, ϵ_0 is the permittivity of free space, $\tan \delta$ is the loss tangent, and $|E_p|$ is the magnitude of the peak field, which is a function of the spatial coordinates. A mathematical representation of $|E_p|$ can be obtained if the waveguide propagation mode is known. For the gyrotron tubes considered here, wave propagation is generally restricted to the transverse electric mode, TE_{02} , in which case $|E_p|^2$ has the form [9, 10]:

$$|E_p|^2 = [E_0 J_1(k_c r) \Phi(z)]^2, \quad (3)$$

where E_0 and k_c are constants for a given power level and frequency. $J_1(k_c r)$ is the first-order Bessel function of the first kind, and $\Phi(z)$ is a periodic function due to multiple reflections at dielectric interfaces. Derivation of $\Phi(z)$ is given in [11]. Since $|E_p|$ and thus q''' depend only upon r and z for TE_{02} mode propagation, the $\partial^2 T / \partial \theta^2$ term in Equation 1 can be eliminated. In spite of this simplifying step, the heat equation is most easily solved using numerical techniques.

Once the temperature distribution $T(r, z)$ is known, the radial and tangential thermal stresses, σ_r and σ_t , respectively, can be determined. Since the temperature distribution depends in a complex fashion on both r and z , finite-element solutions must generally be sought.

3. Procedure

A generalized heat conduction computer code designated HEATING 5, [12] developed at Oak Ridge National Laboratory (ORNL), was used to determine the steady-state temperature distributions.* Individual temperatures were determined at the intersections of a rectangular grid, which consisted of 40 to 50 equally spaced nodes along the radial direction and 10 to 20 equally spaced nodes along the z -axis. The values of the thermal conductivity, k_t , required for the computation were based on information in Table I. The temperature dependence of k_t was also accounted for by including a tabular function composed of individual k_t and temperature values. Linear interpolation was used to determine k_t at temperatures falling between these prescribed quantities.

The window boundaries consisting of two parallel faces and the circumferential edges were assumed to be either insulated or subject to

convective heat transfer. (Heat transfer is indicated by arrows in Fig. 2b.) The heat flow rate, q_b , across uninsulated boundaries was described as

$$q_b = hA(T_s - T_b), \quad (4)$$

where T_b is the temperature of the bulk cooling fluid, T_s is the temperature of the ceramic surface, A is the area normal to the flow direction, and h is the heat transfer coefficient [7]. The h value for the FC-75 was based upon previous heat transfer analyses of the window geometry [13]. As indicated below, a slight temperature dependence of h was also assumed.

A summary of all cases analysed for the TE_{02} mode is given in Table II. Values of the window thickness z_0 were chosen such that the reflection coefficient associated with power output in the gyrotron was minimized [4]. Therefore z_0 was typically a multiple half wavelength in the region. Furthermore, the dielectric properties ϵ_r and $\tan \delta$ for the specific BeO and Al_2O_3 ceramics (Table III) were based on recent dielectric measurements [14]. A constant power throughput of 200 kW was used for all steady-state problems. In Cases 1a to c and 2a to c, the window radius, R_0 , was equal to the waveguide radius, R_w ($= 3.175$ cm). However, subsequent calculations were also performed using R_0 values of 3.81, 5.08 and 7.62 cm (3, 4, and 6 in. diameter windows). The primary motivation was to determine if the maximum tensile stresses could be reduced by the increased constraint offered by the larger diameter windows. A face-cooled Al_2O_3 window operating at 200 kW and 60 GHz was considered for this analysis (Cases 3a to c).

The heat transfer coefficient for the FC-75 used in Cases 1 to 3 was given as

$$h = 0.03 + 0.007(T_s - T_b) \text{ W cm}^{-2}, \quad (5)$$

where T_b was taken as 30°C . This h value was based on an FC-75 flow velocity of ~ 4.57 m sec^{-1} (15 ft sec^{-1}) [13]. The effect of enhancing the heat removal rate upon the resulting tensile stresses for Cases 1 and 2 was also considered. In these analyses (Cases 4 and 5 in Table II) both an increase in the FC-75 flow velocity and a decrease in T_b (to reflect precooling of the FC-75) were considered. The corresponding value of h was

*Because of symmetry, the temperature and stress profiles were determined for only one window in the dual window system (Fig. 2).

TABLE II Summary of microwave window analyses*

Case	Material	$f(\text{GHz})$	$R_0(\text{cm})$	$z_0(\text{cm})$	$h(\text{W cm}^{-2})$
1a	Al ₂ O ₃	28	3.175	0.2189	Eq. 5
1b	Al ₂ O ₃	60	3.175	0.2424	Eq. 5
1c	Al ₂ O ₃	100	3.175	0.2515	Eq. 5
2a	BeO	28	3.175	0.2095	Eq. 5
2b	BeO	60	3.175	0.2095	Eq. 5
2c	BeO	100	3.175	0.2095	Eq. 5
3a	Al ₂ O ₃	60	3.81	0.2424	Eq. 5
3b	Al ₂ O ₃	60	5.08	0.2424	Eq. 5
3c	Al ₂ O ₃	60	7.62	0.2424	Eq. 5
4a	Al ₂ O ₃	28	3.175	0.2189	Eq. 6
4b	Al ₂ O ₃	60	3.175	0.2424	Eq. 6
4c	Al ₂ O ₃	100	3.175	0.2515	Eq. 6
5a	BeO	28	3.175	0.2095	Eq. 6
5b	BeO	60	3.175	0.2095	Eq. 6
5c	BeO	100	3.175	0.2095	Eq. 6

*In all cases $R_w = 3.175 \text{ cm}$.

expressed as

$$h = 1.0 + 0.0099 (T_s - T_b) \text{ W cm}^{-2} \quad (6)$$

with $T_b = 10^\circ \text{ C}$.

The thermal stress distributions were determined using a finite element computer program ADINA [15]. For this calculation, the window cross-section from $r = 0$ to $r = R_0$ was divided into 65 rectangular elements with five elements along the z -axis and thirteen along the r -axis.* Each element contained eight nodes. Values of the thermal expansion coefficient and Young's modulus were taken from Table I.

The ceramic windows also experienced mechanical loading due to pressurization of the FC-75 liquid. This pressure, which was $\sim 206.8 \text{ kPa}$ gauge (30 psig), was required to maintain the necessary flow velocity between the two windows. The distribution of mechanical stresses resulting from the pressure differentials across the window were estimated from well-established expressions describing bending of a circular plate [16].

4. Results and discussion

4.1. Face-cooled windows: Cases 1 and 2

The steady-state temperature-radius profiles obtained for the Al₂O₃ and BeO windows are shown as a function of f in Fig. 3. For each material and frequency, the radial temperature distribution is given for both the vacuum ($z = 0$)

and FC-75 faces ($z = z_0$). It is apparent that the relationship between q''' and r as expressed by Equations 2 and 3 leads to strong radial dependence of the temperature. Further, the positions of the two maxima in the temperature profiles correspond approximately to the maxima in the Bessel function (Equation 3) as one might expect.

The data in Fig. 3 also reveal a significant dependence of the temperature distributions upon f . For example the maximum temperatures and temperature gradients in both BeO and Al₂O₃ became significantly larger as f increases. This behavior results from the frequency dependency of both the heat generation rate (Equation 2) and the loss tangent (Table III). The fact that the increase in T with increasing f is substantially larger for Al₂O₃ primarily reflects the lower thermal conductivity for this material (Table I).

The distributions of the tangential thermal stresses, σ_t obtained for Al₂O₃ and BeO face-

TABLE III. Summary dielectric data for Al₂O₃ and BeO

Material	$f(\text{GHz})$	ϵ_r	$\tan \delta (\times 10^4)$
BeO	28	6.682	8.50
	60	6.680	10.5
	100	6.079	15.0
Al ₂ O ₃	28	9.605	2.80
	60	9.603	4.50
	100	9.600	6.00

*Only the r - z plane is considered in the stress computation since T does not depend upon θ .

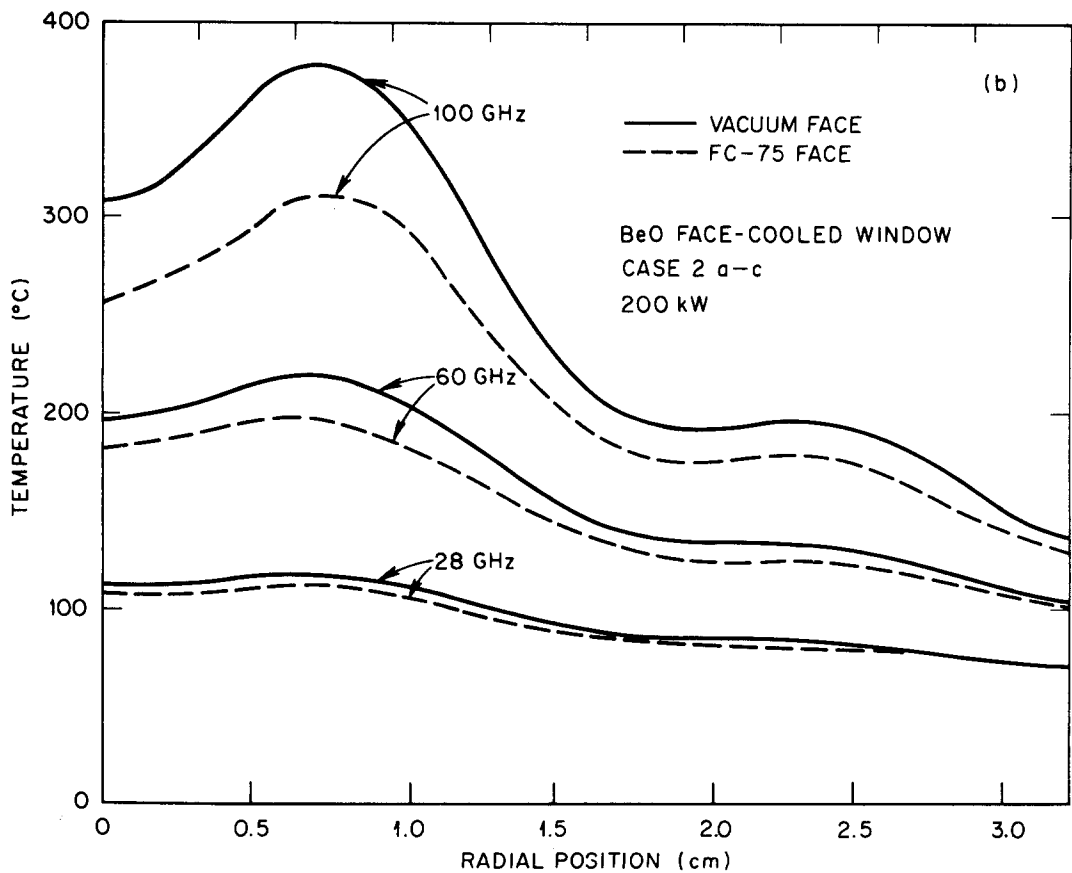
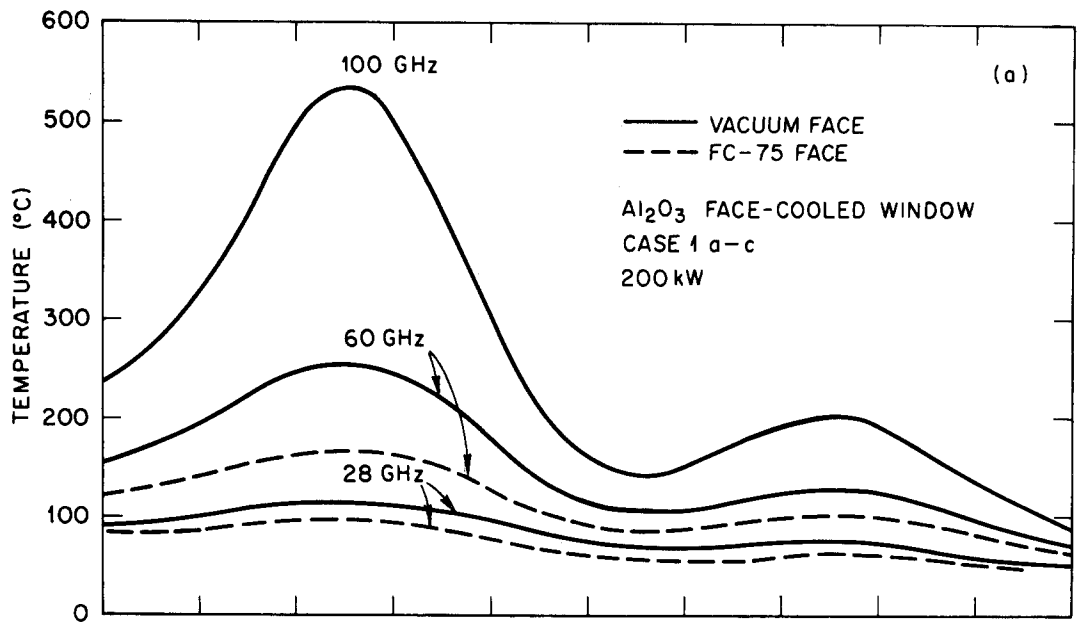


Figure 3 Frequency dependence of radial temperature profiles in (a) Al₂O₃, and (b) BeO face-cooled windows ($R_o = R_w = 3.175$ cm). The temperature profile along the FC-75 face at 100 GHz (not shown) corresponds approximately to the vacuum profile at 60 GHz.

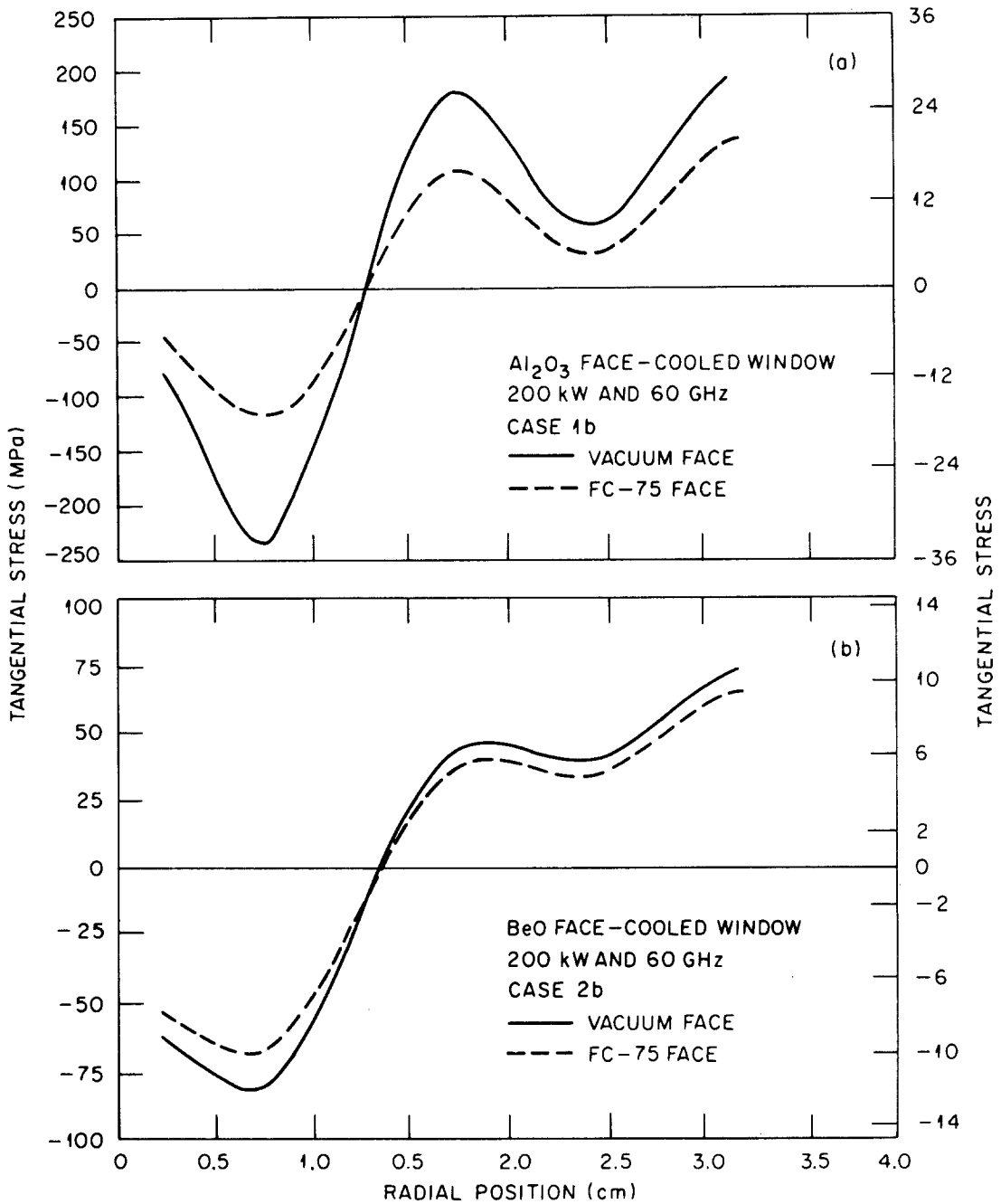


Figure 4 Radial dependence of tangential thermal stresses in (a) Al_2O_3 and (b) BeO face-cooled windows ($R_0 = R_w = 3.175$ cm).

cooled windows at 60GHz are shown in Fig. 4.* It is apparent that the axial variation of σ_t is minor compared with the radial dependence. Such behaviour is to be expected in view of the strong radial temperature dependence (Fig. 3). Furthermore, the maximum tensile stresses for

both materials are generated at the outer window edge, primarily in response to the large radial temperature gradients. Since these gradients are ignored in one-dimensional (through-the-thickness) analyses, the estimated values of maximum stress will not reflect realistic gyrotron operating con-

*The radial thermal stresses are neglected in the subsequent discussions because they are compressive throughout the window and thus, are assumed not to contribute to window failure.

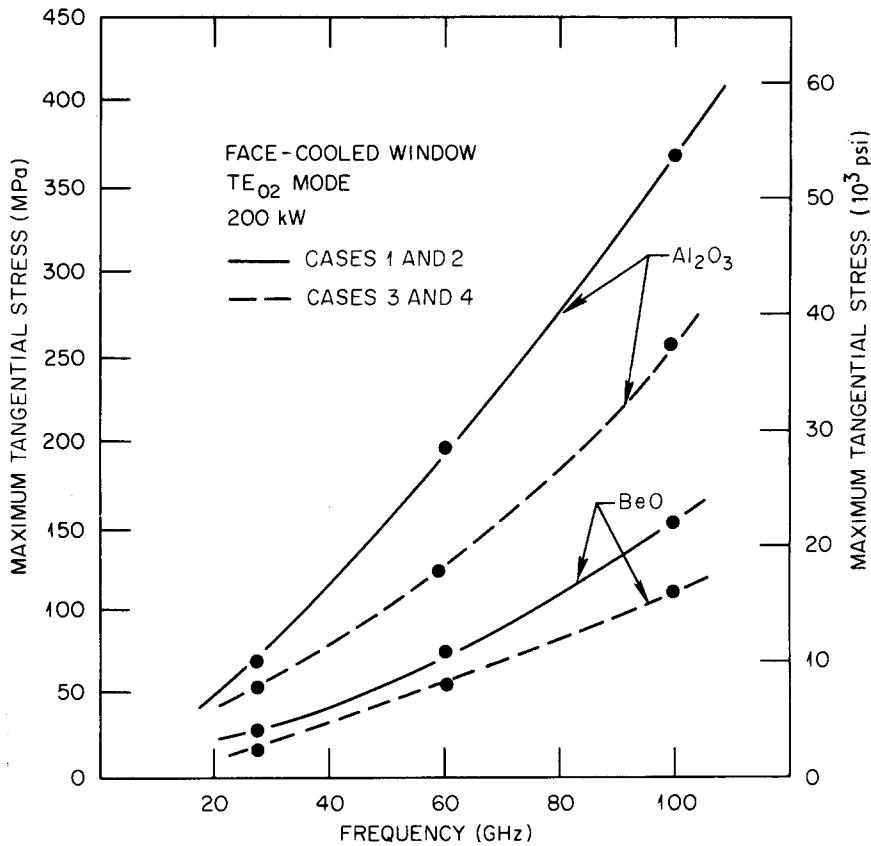


Figure 5 Variation of maximum tangential stress with frequency for Al_2O_3 and BeO face-cooled windows. Dotted lines are for conditions of enhanced convective heat transfer.

ditions. For example, a one-dimensional treatment [17] for Al_2O_3 and BeO at 60 GHz, predicts maximum stresses of 103 MPa (15×10^3 psi) and 32 MPa (4.7×10^3 psi), respectively. The quantities are significantly less than the corresponding values in Fig. 4.

The values of the maximum tangential stresses σ_t^m are given as functions of f in Fig. 5 (solid lines). The fact that σ_t^m for Al_2O_3 is significantly greater than for BeO (at a given frequency) is primarily a consequence of the larger temperature gradients in the former material. For frequencies above 60 GHz, σ_t^m for both materials represents a significant fraction of the inert fracture strengths (Table I). As discussed in Part 2, these results suggest that time-dependent window failure is a distinct possibility under these gyrotron operating conditions.

The previous stress profiles ignore the contribution of mechanical stresses arising from pressure

differentials across the window. The nature of these stresses occurring along the vacuum face is illustrated in Fig. 6 for the case of a window simply supported at $R_w = 3.175$ cm ($z_0 = 0.2$ cm) and subjected to a 310 kPa (45 psi) pressure differential.^{†‡} The tangential and radial stresses (σ_t and σ_r , respectively) reach maximum values at the window centre where $\sigma_t = \sigma_r = 95.3$ MPa (13.8×10^3 psi). Fortunately, these large tensile mechanical stresses are opposed by the compressive thermal stresses generated during gyrotron operation (Fig. 4). The nonzero value of σ_t (mechanical) at $r = R_w = 3.175$ cm will also enhance the tensile thermal stresses near the window edge. Therefore, reliable estimates of the window stresses require that one combine both the mechanical and thermal stress profiles.

The previous stress distributions strongly suggest that window failures will occur at the outer edge. This conclusion has been substantiated

[†] Represents a FC-75 gauge pressure of 206.8 kPa (30 psi).

[‡] The stress distribution in Fig. 6 is for either BeO or Al_2O_3 .

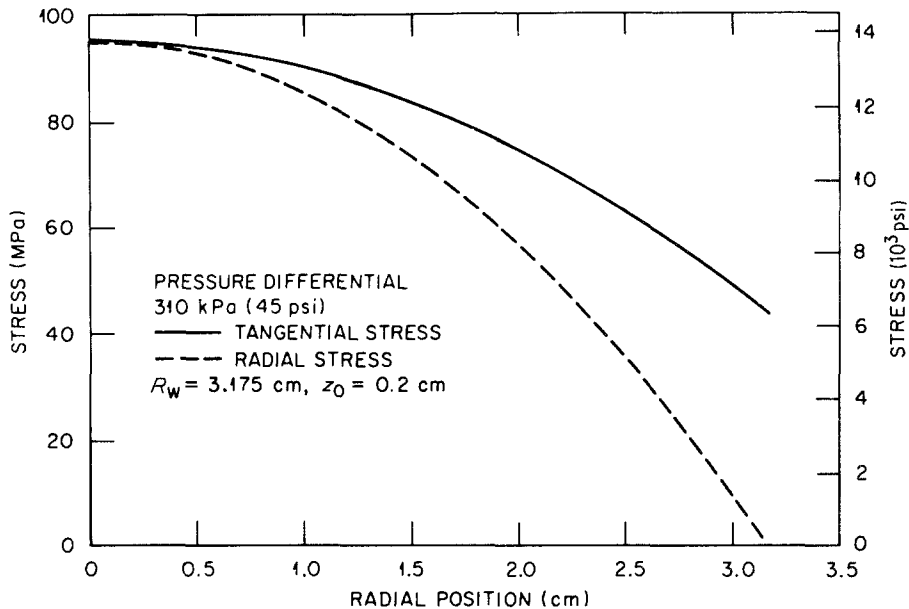


Figure 6 Distributions of tangential and radial stresses along vacuum face resulting from FC-75 pressure loading.

by direct observations of fractured windows. For example, Fig. 7 illustrates a typical fracture pattern in a failed BeO window. As indicated by the arrows, the crack starts at the window edge and then proceeds toward the window centre where it branches into two main cracks. Additional branching also occurs near the failure origin. The propagation of the crack toward the window centre would at first seem to be quite unlikely in view of the high compressive stresses in the region. However, as the crack advances, the loss of constraint of the cracked material will cause the tensile stresses to be shifted toward the centre region.

4.2. Effect of window radius and heat transfer coefficient: Cases 3–5

The effect of window radius upon the tangential stress profiles (along the vacuum face) is illustrated in Fig. 8 for a face-cooled Al_2O_3 window operating at 60 GHz (Case 3). These data reveal a significant reduction in the maximum stress from 193 MPa (28×10^3 psi) to 102 MPa (14.8×10^3 psi) as the window radius is increased from 3.81 cm (1.5 in.) to 7.62 cm (3.0 in.). The larger diameter window essentially provides additional constraining action against the thermal expansion of the central region. Since the tensile stresses are distributed over a greater portion of the window, the peak stress is reduced. This concept

of constraining the thermal expansion could be carried a step further by using an outer ring to compressively load the window. The ring material would have to be sufficiently strong to support the tensile stresses as well as be resistant to slow crack growth effects. Although a metal retention ring would satisfy these requirements, other problems related to excitation of ghost modes in the waveguide might arise [11]. Consequently, a ceramic material such as silicon nitride might be a more suitable candidate for the retention ring.

Although not indicated above, the window thickness, z_0 , can also significantly influence the window stresses. For example, a decrease in z_0 will lower the total heat generated within the window. This will lead to a reduction in both the axial and radial gradients, thereby lowering the maximum thermal stress. However, the mechanical stresses, which are proportional to z_0^{-2} , will increase with decreasing thickness. This tradeoff must be considered before substantial reductions in z_0 are made.

The effect of enhancing the heat transfer coefficient h upon the maximum tensile stresses generated in Al_2O_3 and BeO is illustrated in Fig. 5 (dotted line). The increased heat removal rate leads to significant reductions in the tangential thermal stresses associated with both materials. The implications of these reduced service stress

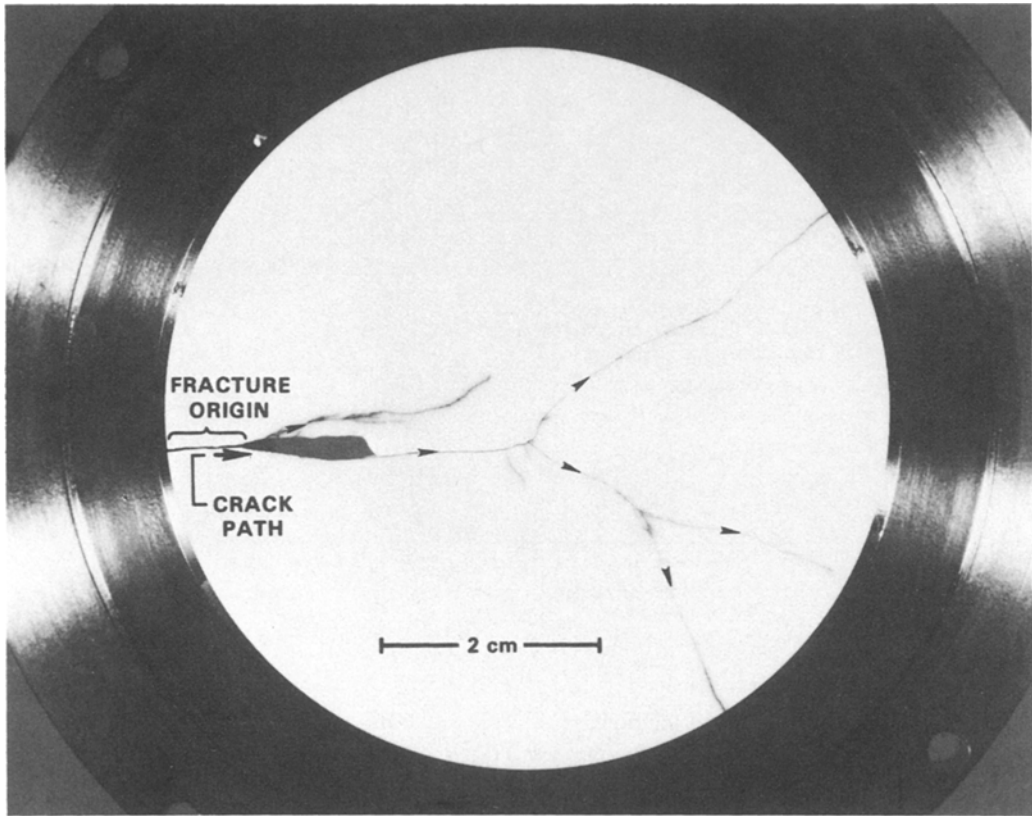


Figure 7 Failure origin in fractured BeO window.

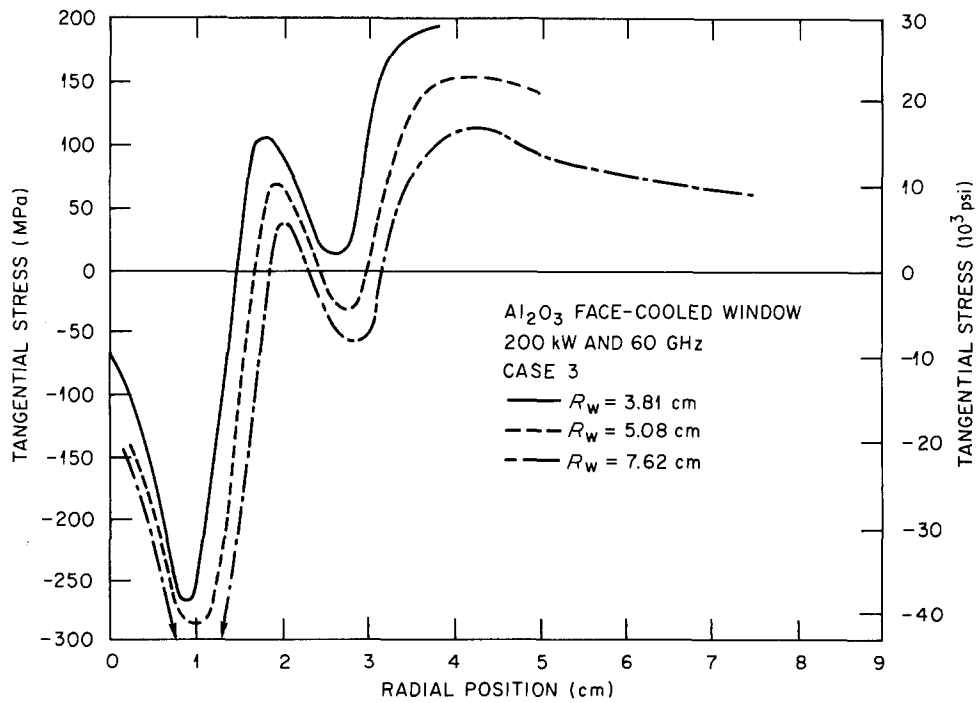


Figure 8 Effect of window radius upon tangential stress distribution along vacuum side of face-cooled Al₂O₃ window.

levels upon the long-term mechanical reliability are discussed in Part 2. Finally, it should be mentioned that the larger flow velocities required to enhance h also result in greater pressure differentials across the window and thus higher mechanical stresses. This will place practical limits on maximum obtainable heat transfer coefficient.

5. Conclusions

Because of the simple geometry of current gyrotron windows, a closed form solution was derived for the 3-D electric field inside the windows. From this field, using finite-element computer codes, estimates of thermal stress were obtained for both the Thermalox 995 standard BeO and the Al 995 Al₂O₃ ceramics at 28, 60, and 100 GHz for power levels of 200 kW.

The results show that large radial temperature gradients are responsible for the maximum tensile stress that occurs at the window outer edge in all cases studied. At frequencies much above 28 GHz with 200 kW input power, the edge tensile stresses become a significant fraction of the inert fracture strength. Although not conclusive, the available data on failed gyrotron windows tend to substantiate these results.

Window designs should be sought which maximize thermal transfer coefficients from ceramic to coolant interfaces and which minimize the edge tensile stresses (i.e., higher flow velocities and larger diameter windows or a retention ring).

Acknowledgement

Research sponsored by the Office of Fusion Energy, US Department of Energy, under contract W-7405-eng-26, with the Union Carbide Corporation.

References

1. J. C. GLOWIENKA, *J. Vac. Sci. Technol.* **18** (1981) 1088.
2. C. P. MOELLER, "Launchers and Transmission Systems for Electron Cyclotron Heating", GA-A16690, General Atomic Company, San Diego, California, March (1982).
3. P. F. BECHER and M. K. FERBER, "Mechanical Reliability of Current Alumina and BeO Ceramics Utilized in Microwave Windows for Gyrotrons", ORNL/TM-8555, Union Carbide Corp. Nuclear Division, Oak Ridge National Laboratory, Tennessee, USA.
4. S. M. WIEDERHORN, *Int. J. Fract. Mech.* **4** (1968) 171.
5. J. B. WACHTMAN, Jr, *J. Amer. Ceram. Soc.* **57** (1974) 509.
6. P. F. BECHER, M. K. FERBER and V. J. TENNERY, "Mechanical Reliability of Ceramics for Microwave Window Application", ORNL/TM-7811, Union Carbide Corp. Nuclear Division, Oak Ridge National Laboratory, Tennessee, USA, July (1981).
7. H. S. CARSLAW and J. C. JAEGER, "Conduction of Heat in Solids", 2nd Edn (Clarendon Press, Oxford, 1959).
8. L. H. VAN VLACK, "Materials Science for Engineers" (Addison-Wesley, Reading, Mass., 1970) pp. 262-3.
9. S. RAMO, J. R. WHINNERY and T. V. DUZER, "Fields and Waves in Communication Electronics", (Wiley, New York, 1965) pp. 429-34.
10. R. F. HARRINGTON, "Time-Harmonic Electromagnetic Fields", (McGraw-Hill, New York, 1961) pp. 198-250.
11. M. F. FERBER, H. D. KIMREY and P. F. BECHER, "Analysis of the Temperature and Stress Distributions in Ceramic Materials Subjected to Microwave Heating", ORNL/TM-8718, Union Carbide Corp. Nuclear Division, Oak Ridge National Laboratory, Tennessee, USA, July, (1983).
12. W. D. TURNER, D. C. ELROD and I. I. SIMANTOV, "An IBM 360 Heat Conduction Program", ORNL/CSD/TM-15, Union Carbide Corp Nuclear Division, Oak Ridge National Laboratory, Tennessee, USA, March (1977).
13. G. HU, Varian Associates, Palo Alto, California, USA, personal communication.
14. M. N. AFSAR and K. J. BUTTON, *IEEE Trans. Microwave Theory Tech.* **31** (1983) 217.
15. KLAUS-JURGEN BATHE, ADINA (computer program), Massachusetts Institute of Technology, Cambridge (1978).
16. S. P. TIMOSHENKO and J. N. GOODINER, "Theory of Elasticity" (McGraw-Hill, New York, 1970) pp. 385-8.
17. H. R. JORY, E. L. LIER and R. S. SYMONS, "Final Report Millimeter Wave Study Program", ORNL/Sub-75/49438/2, Union Carbide Corp. Nuclear Division, Oak Ridge National Laboratory, Tennessee, USA, November (1975).
18. W. W. HO, "High Temperature Millimeter Wave Characterization of the Dielectric Properties of Advanced Window Materials", SC5235. 17 FRD, Rockwell International Science Center, Thousand Oaks, California, USA (1981).

Received 20 January
and accepted 30 January 1984